Polym. Bull. (2010) 65:753–766
DOI 10.1007/s00289-009-0242-9

ORIGINAL PAPER

The effect of chain extenders structure on properties of new polyurethane elastomers

Stefan Oprea

Received: 25 May 2009 / Revised: 18 November 2009 / Accepted: 22 December 2009 /
Published online: 9 January 2010

Abstract Two series of polyurethane elastomers were synthesized to investigate what effect does the incorporation of various new chain extenders have on the mechanical and thermal properties of polyurethane elastomers. The polyurethane soft segments were based on poly(ε-caprolactone) polyol. The hard segment was based on 1,6-hexamethylene diisocyanate in combination with 2,5-dimethyl-3-hexine-2,5-diol (DHD), hexaethylene glycol, glycerin, or castor oil. The results showed that the degradation rate and mechanical properties of the final products can be controlled through the structure of diol chain extenders or/and hard segment cross-linking present in the polyurethane elastomers. The DHD-based polyurethane displayed a relatively low glass transition temperature of −57 °C and a tensile strength of 11–14 MPa and elongation at break of 600–700%. These kinds of materials have potential application in many domains.

Keywords Polyurethane elastomers · Chain extenders · Cross-linker · Mechanical properties

Introduction

Polyurethanes (PUs) are an important class of materials with wide application such as in coatings, binder resins, fibers, and high-performance elastomeric products. PU elastomers are multiblock copolymers and exhibit good elasticity even with a wide variation of hardness. The thermodynamic incompatibility between hard and soft segments leads to microphase separation, which is responsible for the excellent elastomeric properties of PUs. Microphase separation, as well as the chemical

S. Oprea (✉)
"Petru Poni" Institute of Macromolecular Chemistry, Aleea Grigore Ghica Voda No. 41-A, 700487 Iasi, Romania
e-mail: stefop@icmpp.ro

structures of soft and hard segments, the types of extender cross-linked reagents that were used, crosslink density and reaction conditions all strongly influence the mechanical properties and thermal stabilities of PU elastomers [1–5]. Choosing a suitable diisocyanate and chain extender results in various influences on the final properties of PUs. Mechanical properties of PU elastomers depend strongly on the ratio of hard and soft segments and the structure or length of chain extenders [6, 7].

For potential utility in biomedical applications it is required to obtain good biocompatibility and low hydrolytic and enzymatic degradable tendency. In order to do so, PUs are generally synthesized with soft segments such as poly(ε-caprolactone), poly(ester)diol and poly(carbonate)diol and aliphatic diisocyanates which provide better light stability and better resistance to hydrolysis and thermal degradation [8–16]. Hard segments usually exhibit inter-chain interactions which determine the strength of the hard segment and thus the macroscopic properties. A large amount of hard segment in polymer structure leads to determine higher hardness and glass transitions [17–19].

It is well-known that inter-urethane hydrogen bonding between the carbonyl and N–H groups and microphase composition are important parameters for designing biodegradable materials [9, 20]. The distribution of hydrogen bonds can be disturbed by the existence of a branched structure of the chain extender or by chemical cross-links that impeded the free movement of macromolecular chains.

This work describes the catalyst-free synthesis of PUs with various new hard segments with 1,6-hexamethylene diisocyanate (HDI) and poly(caprolactone) (PCL) as soft segment. It evaluates the effect that the variation of the chain extending diols' structure and the cross-linkers' nature have on the thermal and mechanical properties. This new group of PUs shows good mechanical properties and processability.

Experimental

Materials

HDI provided by Fluka was used as received. The polydiol was PCL. This polymer was provided by Aldrich. The polydiol average molecular weight is 2,000 g/mol. The chain extenders: 2,5-dimethyl-3-hexine-2,5-diol (DHD) [linear formula: $HO–C(CH_3)_2–C\equiv C–C(CH_3)_2–OH$] and glycerin (Gly) were provided by Aldrich, hexaethylene glycol (HEG) [linear formula: $H(OCH_2CH_2)_6OH$] was provided by Fluka, castor oil (CO) provided from Aldrich and were used as received. Polyester and chain extenders were dried under a vacuum until the content of water was below 0.03%.

Methods

Synthesis

As usually done, the synthesis of PU was done by the following procedure and the moles of added reagents for the various PU are shown in Table 1.

Table 1 Formulations of the obtained polyurethanes

Designation samples	Molar ratio PCL/HDI/ chain extenders	Chain extenders
PU1	1:2:1	2,5-Dimethyl-3-hexine-2,5-diol
PU2	1:2:1	Glycerin + 2,5-dimethyl-3-hexine-2,5-diol
PU3	1:2:1	Castor oil + 2,5-dimethyl-3-hexine-2,5-diol
PU4	1:2:1	Hexaethylene glycol
PU5	1:2:1	Glycerin + hexaethylene glycol
PU6	1:2:1	Castor oil + hexaethylene glycol

The PUs were synthesized in a two-step polymerization procedure. The average hard segment (HS) composition was controlled by the molar ratios of poly-diol/HDI/diol and triol of chain extenders and by the nature of diol and triol used in the synthesis. The OH_{diol}/OH_{triol} ratio used was of 1/1 in each of the synthesized PU samples. The synthesis of PUs was performed in a 500 mL glass reactor at normal pressure, under a nitrogen blanket and vigorous agitation. The NCO/OH ratio of all formulations was shown in Table 1.

Polyester diol was reacted with a diisocyanate at 80 °C for 2 h, in order to yield a prepolymer that was mixed in the second step with chain extenders at 80 °C for 10 min. The progress of the reaction was monitored by measuring the infrared absorption of the isocyanate band at 2,200–2,300 cm^{-1} and the reaction was considered to be complete when this band disappeared. The resulting material was poured into a mold and left to cure at 80 °C for 20 h. Under these conditions, the addition of catalysts was not necessary. PU sheets thus prepared were used for the determination of mechanical and physical properties and for the thermal resistance study.

Measurements

The FTIR spectra were recorded on a Bruker VERTEX 70 Instruments equipped with a Golden Gate single reflection ATR accessory. The spectra were recorded in the range of 600–4,000 cm^{-1} with a nominal resolution of 4 cm^{-1}.

The thermal stability of PUs was tested in an air atmosphere by thermogravimetric analysis (TGA) using a DERIVATOGRAF Q-1500 D apparatus (Hungary). The rate of TGA scans was 10 °C/min. The initial weight of the samples was about 50 mg and the temperature range was 30–700 °C.

A differential scanning calorimeter (DSC) type DSC-7 Perkin-Elmer was used for thermal analysis and was operated at a heating rate of 10 °C/min. The thermal transition behavior was studied using measurements involving a temperature range of −100 to 100 °C. Tests were conducted on samples of about 10 mg exposed to a gradual heating procedure in order to observe the glassy transition temperature (T_g).

Dynamic mechanical analysis (DMA) was performed using a Perkin-Elmer Diamond DMA to determine the storage modulus (E') and the loss factor (tan δ). All samples were scanned from a temperature sweep of −100 to 200 °C at a constant

heating rate of 2 °C/min. The resulting plots for E' and tan δ are displayed as a function of frequency at 1 Hz.

Stress–strain measurements were performed on dumbbell-shaped samples cut from the obtained PU sheets. The tests were performed at room temperature using a Shymadzu EZTest (Japan), equipped with a 5 kN load cell. The used cross-head speed was 50 mm/min. At least five identical dumbbell-shaped specimens for each PU sheet were tested, and their average mechanical properties were reported.

Contact Angle Measurements (CA) were performed using deionized water and ethylene glycol droplets of 5 μL over the different neat PUs surfaces' using a Dataphysics Contact Angle System KSV Instruments LTD, Finland. Water CA measurements were acquired using the sessile drop method [21]. The CA was measured within 45–60 s of the addition of the liquid drop with an accuracy of ±1°. Measurements were repeated six to ten times with different test pieces of the same PU type to check the accuracy.

Results and discussions

FTIR spectroscopy was used to investigate the structural differences of the hard segments of PU elastomers synthesized.

The FTIR spectra of the two PU series with different hard segment structures are shown in Figs. 1, 2.

The infrared research on PUs has focused on two principal vibration regions: the N–H stretching vibration (3,200–3,500 cm^{-1}) and the carbonyl C=O stretching vibration in the amide I region (1,690–1,730 cm^{-1}). PUs are capable of forming several kinds of hydrogen bonds due to the presence of a donor N–H group and a C=O acceptor group in the urethane linkage [22]. These bands have been widely used to characterize the hydrogen bonding state of the polymer, and was used in correlation with the phase separation in the system. It is well-known that in

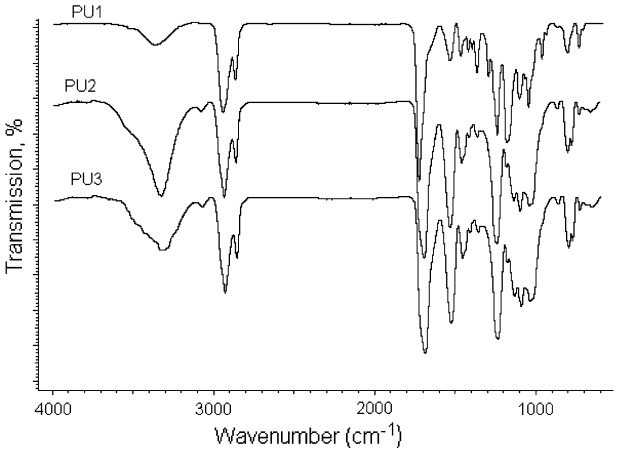

Fig. 1 FTIR spectra of polyurethane elastomers synthesized with DHD

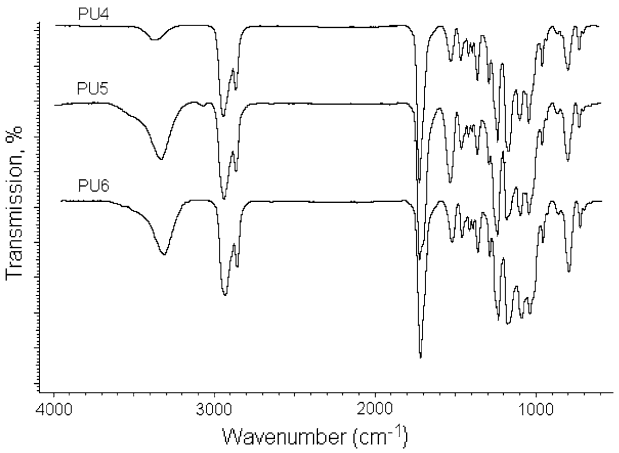

Fig. 2 FTIR spectra of polyurethane elastomers synthesized with HEG

hydrogen-bonded urethanes, N–H and C=O bands appear at lower wave numbers than the bands that appear in urethanes free from hydrogen bonding [22–24]. In the case of HEG–PU elastomers, the appearance of a single N–H band at 3,300 cm^{-1} suggested that most of its N–H groups were hydrogen bonded. In the case of DHD-based PU, an N–H absorption band was found at 3,330 cm^{-1}, indicating a much lower tendency to form hydrogen bonds than the PUs formed with HEG. This is due to a steric-hindrance effect caused by the branched chains appearing in DHD, which block the formation of hydrogen bonds. Cross-linked PUs elastomers show an enlarged area of absorption band at 3,300 cm^{-1} and this suggests that the degree of hydrogen bonding between hard segment and soft segment is low.

TGA is the most favored technique for the evaluation of the thermal stability of polymers. TGA curves of the PU elastomers with various chain extenders are shown in Figs. 3, 4.

For PU1, PU2, and PU3 the weight loss was very slow until 300 °C, followed by a rapid increase of weight loss that ended approximately at 450–500 °C. For PU4, PU5, and PU6 the decompositions started approximately at 250 °C. In the temperature range of 300 to 500 °C it was found that the weight loss curves of DHD–PU were similar among each other, while those of HEG–PU exhibited differences from one curve to the other.

TGA data for PU4, PU5, and PU6 reveal different degradation processes correlated with the structure of the hard segments. The PU based on CO had its fastest rate of loss at 250 °C, while the PU based on Gly had its fastest rate of loss at 350 °C. The weight loss of the PU based on CO takes place at lower temperature, which is in accordance with the existence of the plasticizing effect of the dangling chains of CO. The presence of HEG in the chemical structure of the PU (linear chain extender and high amount of hydrogen bonding in PU chains) results in a switch of the beginning of degradation from 250 to 235 °C. The main degradation process can be observed at temperatures around 400 °C.

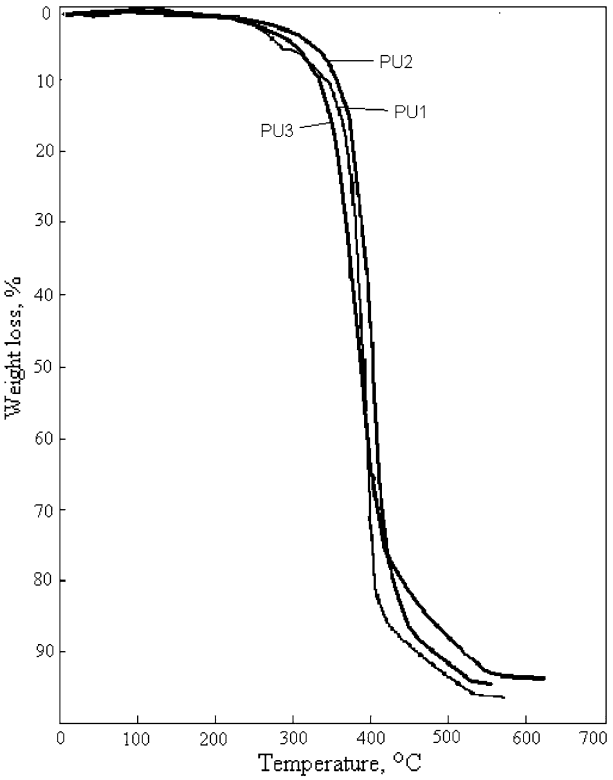

Fig. 3 TGA curves of DHD-based polyurethane elastomers

In the TG curve of PUs, a maximum is present at about 380–410 °C for PUs with DHD and at 330–400 °C for PUs with HEG.

The increase of the maximum temperature for cross-linked PU indicates a lower rate of diffusion of the degraded products within of the matrix.

DSC thermograms obtained for the different PUs in a range between −100 and 100 °C are shown in Figs. 5, 6.

For these HDI-based PUs, glass transition values indicate the importance of the hard segment on the PU composition. In this case, the difference is due to the differences in the chain extender used. The changes in T_g are attributed to a certain degree of phase mixing of hard and soft segments. It is known that (physical) cross-links can have a major influence on the soft segment's T_g [12]. For DHD-based PUs, glass transition values ($T_g = -57$ °C) indicate the presence of small physical cross-links between the hard segments of the PU. The lower T_g is an indication for the existence of better phase separation. From thermal data for HEG-based PUs, it can be observed that they exhibit higher glass transition temperatures ($T_g = -44$ °C) than those of DHD-based PUs with the same hard segment content. The transition that was observed could be explained through the hindering effect of the more ordered hard segment structures on the chain extenders' mobility. The fixation of

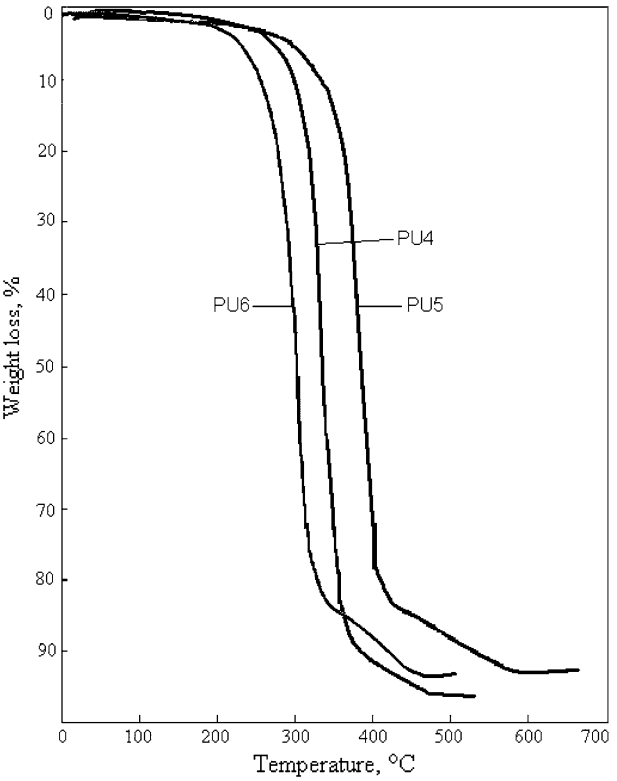

Fig. 4 TGA curves of HEG-based polyurethane elastomers

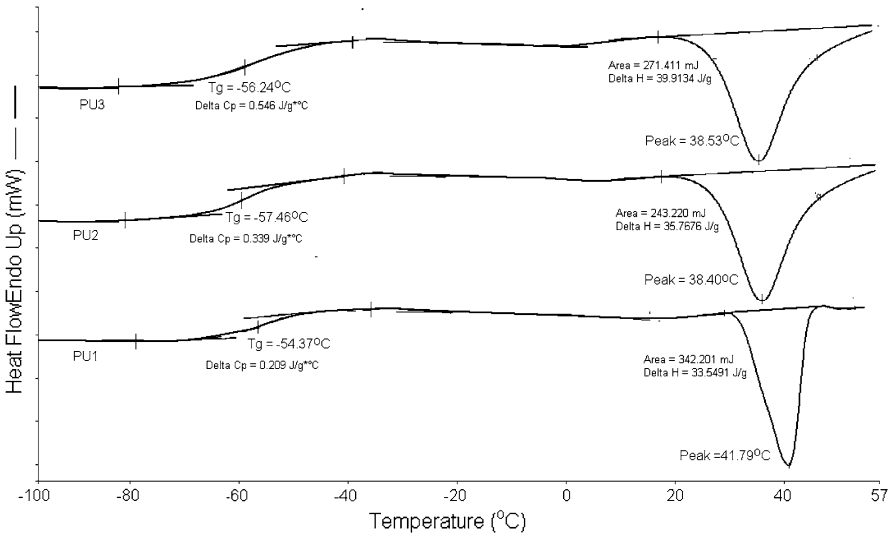

Fig. 5 The DSC scan plots for polyurethane based on DHD

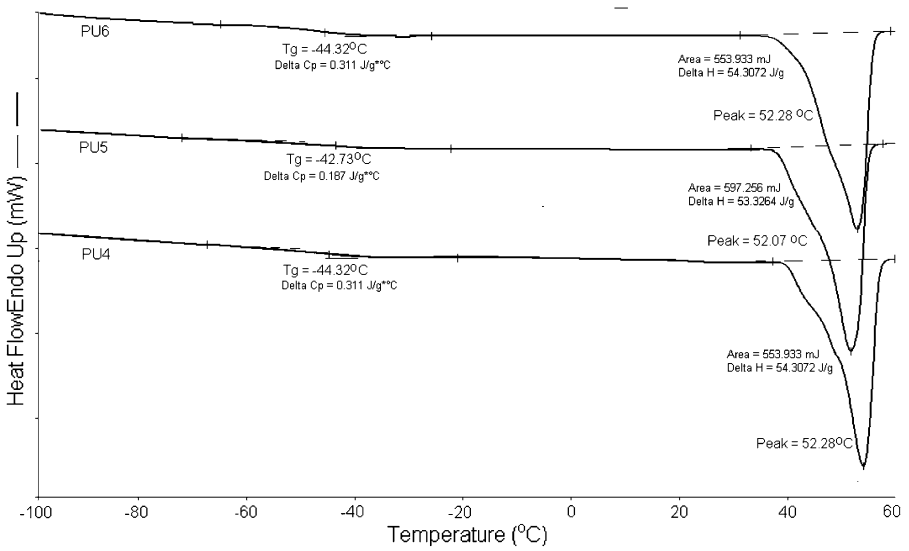

Fig. 6 The DSC scan plots for polyurethane based on HEG

the hard blocks by chemical cross-linking made the glass transition temperature be lower for DHD-based PUs. It was attributed to the reduction of chain mobility and the effect of branched chain extender that hinders the formation of hydrogen bonds. HEG-based PUs have relatively similar soft segment T_g for the various hard segment structures and higher values ofT_g are an indication that there is some mixing of hard segments in the soft segment domain [25]. The more ordered hard segment structures that are formed by chemical cross-linking have a mobility-hindering effect on the soft segments, which leads to having less soft segment-ordered structures or crystals.

DMA of the molded PUs provides information on viscoelastic properties. The elastic modulus (E') and loss tangent (tan δ) of the DHD- and HEG-based PUs with different hard segment cross-links in the temperature range from −100 to 230 °C are shown in Figs. 7, 8.

The elastic modulus (E') shows a decrease at low temperatures (−45 °C) and tan δ shows a peak associated with the glass transition temperature of the soft segment. For PUs based on DHD, E' decreases continually with the increase of the temperature. This means those hard segments are not able to form a sufficient amount of physical cross-links.

For HEG PUs, the modulus curve shows a plateau, which indicates the existence of physical cross-links which increase the size of the inter-connectivity of hard segment domains, resulting in a significant structural reinforcement. This plateau is more extensive for PUs based on Gly cross-linker.

The E' has an abrupt decrease at 50 °C that can be ascribed as melting of the soft segment phases. The E' sharp decreases upon heating at 220 °C for PU based on DHD and at 250 °C for PU based on HEG, indicating that the physical and chemical cross-linking sites between hard segments are totally destroyed [26].

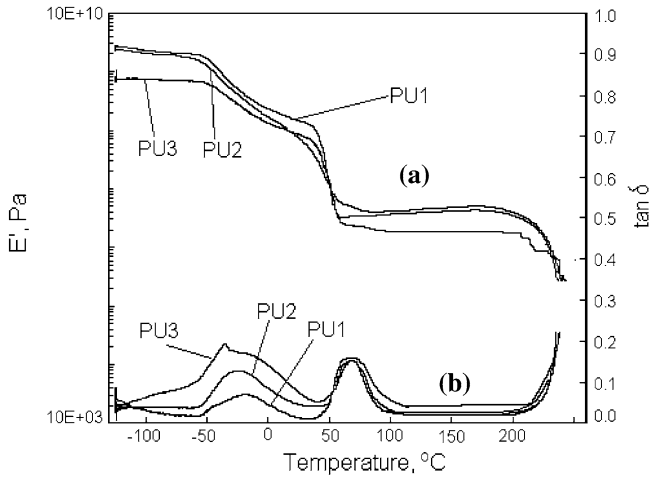

Fig. 7 Typical DMA spectra of the polyurethane samples based on DHD. Storage modulus: E' (*a*), damping: tan δ (*b*)

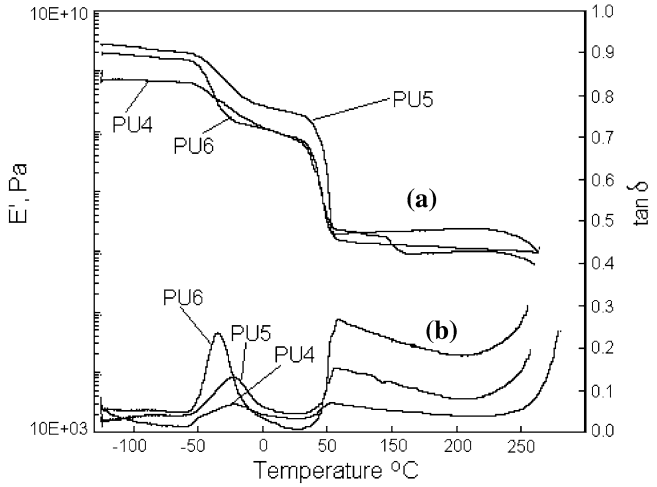

Fig. 8 Typical DMA spectra of the polyurethane samples based on HEG. Storage modulus: E' (*a*), damping: tan δ (*b*)

The mechanical behavior of PU elastomers is dependent on the intermolecular interactions between their hard segments. Stress–strain, modulus, and elongation are important for polymer characterization, and they show how the variation of the diisocyanate and/or chain extender's molecular weight, as well as variation of chain extenders' structure has led to modifications of the PU mechanical properties [5, 27]. The stress–strain curves representing the various chain extender PU elastomers, but with a common soft segment, are grouped in Figs. 9, 10.

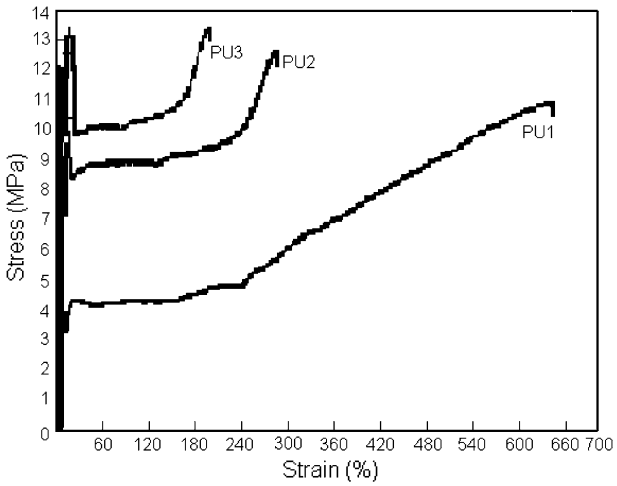

Fig. 9 Stress versus strain curves for the DHD–polyurethane

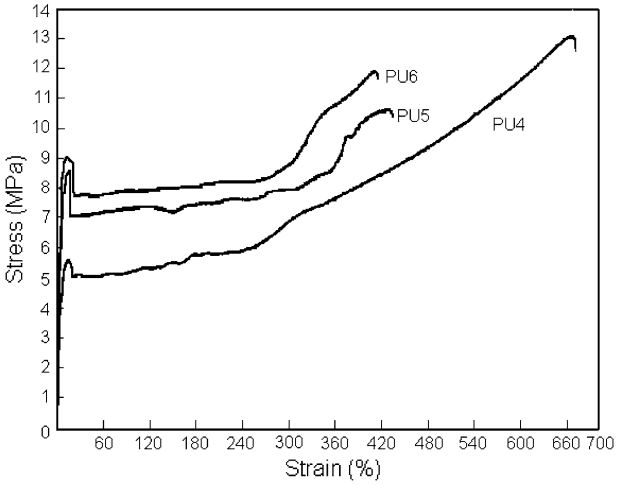

Fig. 10 Stress versus strain curves for the HEG–polyurethane

Three different regimes are visible. The pure elastic deformation appears in the case of low deformations [28]. Second, for all the polymers studied an area of plastic flow appears. Finally, at strains above 300% an increase in the curves can be observed, which can be attributed to strain-induced crystallization of the soft segment chains [12].

In the case of PU with DHD the tensile strength at break is 10.5 MPa and maximum elongation is 650%. PU sheets with DHD and Gly display a tensile strength of 12.5 MPa followed by a decrease and then increase until break. The PU with CO is more rigid, having a tensile strength of 13.5 MPa and elongation at break of 200%.

Cross-linking present in the hard segment structure leads to an increase in stress and a decrease in strain. Uniform soft segments are used and consequently only the hard segments influence the deformation stress.

In the case of the branched chains of the difunctional chain extender, and consequently for a low physical cross-linkage density, there was a decrease in strength. It is clear that the variation of the chain extender structure and the cross-linking nature affect the tensile properties of the cross-linked PU materials.

In segmented PUs, the mechanical properties were generally accredited to a pseudo-cross-linking effect resulting from the HS aggregation. The HS domain generally exhibits a different degree of ordered structure, which was considered to be able to reinforce the hard segment domain and, in the case of these PUs, added a cross-linking effect deriving from the usage of Gly or CO.

The surface hydrophilicity of the various samples was characterized through static water CA. The CA is a quantitative measure of the wetting of a solid by a liquid. Wettability of PU elastomers was examined by CA measurements using two probe liquids, water and ethylene glycol. The droplets of the different pure liquids (distilled water and ethylene glycol) were placed on the solid surface. In order to obtain reproducible results for the CA determinations, several conditions had to be fulfilled, such as: constant temperature during the determinations, same volume of the solvent drops, evaluation of the CAs in different points of the studied surface, and the final result being the average of the obtained values. The precision in evaluating the components of the free surface energy is given by the precision in reading the CAs between the polymer surface and the pure liquids that were used. The hard segment fraction was varied in the PU films' formulation in order to determine its influence on the wettability.

Table 2 shows CAs and the work of adhesion obtained for the different materials depending on the hard segment composition used.

The DHD-based PUs had higher CAs than HEG-based PUs, meaning lower polarity. These variations in CAs can be ascribed to the modification of the degree in which the hard segments interact among themselves and the difference in phase segregation behavior [9]. The DHD-based PUs, poorly phase segregated, provide the materials with a more hydrophobic surface character. The CAs for the PU based on CO + HEG were 10° higher than those of the PU based on HEG. Hydrophobic surfaces are known to inhibit the proliferation and increase the rate of apoptosis of osteoblastic cells compared to cells grown on hydrophilic surfaces [29].

Table 2 Contact angle (θ) and work of adhesion (W_a) values of the polyurethane film surfaces

Sample	Water		Ethylene glycol	
	θ (°)	W_a (mN/m)	θ (°)	W_a (mN/m)
PU1	79	86	62	70
PU2	82	83	71	63
PU3	80	85	45	82
PU4	79	94	77	49
PU5	76	89	69	65
PU6	90	73	75	60

Table 3 Interfacial tension for a solid–liquid system (γ_{sl}) polyurethane elastomers obtained

Sample	λ_{sv}^{p} (mN/m)	λ_{sv}^{d} (mN/m)	γ_{sl} (mN/m)	
			Water	Ethylene glycol
PU1	13.9	12	13	4
PU2	17.4	6	13.5	8.3
PU3	4.4	34.5	27.8	5.4
PU4	3.6	31.7	28.49	6.1
PU5	17.7	9.4	11	5.4
PU6	8.7	10.4	19.5	6.6

p Polar, *d* disperse

The work of adhesion, W_a, was calculated using the following equation:

$$W_a = \gamma_{lv}(1 + \cos\theta), \tag{1}$$

where γ_{lv} is the surface tension of the liquid used for the CA measurement.

The interfacial tension for a solid–liquid system (γ_{sl}) was calculated using the following equation [29, 30]:

$$\gamma_{sl} = \left(\sqrt{\gamma_{lv}^{p}} - \sqrt{\gamma_{sv}^{p}}\right)^2 + \left(\sqrt{\gamma_{lv}^{d}} - \sqrt{\gamma_{sv}^{d}}\right)^2 \tag{2}$$

The resulting interfacial tensions are listed in Table 3.

From Table 3, we can see that the values of the interfacial tension of polymers containing DHD are lower compared to those of the other compositions. Again, for the Gly systems the interfacial tension is slightly lower compared to that of other compositions. The variation of the hard segment structure in the polymer matrix may have also affected the surface properties. Phase segregation and hydrogen bonding provide hardness and hydrophilic character to the materials as proved by hardness and CA measurements.

Conclusions

PU elastomers have been prepared by reacting polyols with terminal primary functional groups with aliphatic diisocyanate. The prepolymers were chain-extended with bifunctional precursor chains and with CO or Gly as a trifunctional cross-linker at stoichiometric ratios.

Longer chain lengths between cross-links produce higher elongations at break and lower mechanical moduli. The branched chains of the difunctional chain extender decrease the physical cross-links density, and thus results a decrease in strength. The cross-linking process increases the urethane domain rigidity and decreases the soft segment crystallinity. These factors enhance the tensile strength of the materials.

The thermal stability is a function of the components present in the formulation. Higher length of the hard segment and the presence of Gly linkages increased the PU's thermal stability. PU based on CO exhibited a T_g decrease of about 12 °C that

resulted from the presence of dangling chains in the triglyceride structures that act as plasticizers.

The DHD–PU displayed a relatively low glass transition temperature of −57 °C and a typical behavior of a PU rubber at room temperature having a tensile strength of 11–14 MPa and elongation at break of 600–700%.

The variation of the hard segment structure in the polymer matrix may also have affected the surface properties.

Acknowledgment The author gratefully acknowledges Dr. Mariana Cristea for her assistance with the DMA measurements.

References

1. Hepburn C (1991) Polyurethane elastomers, 2nd edn. Elsevier, London
2. Zhang H, Chen Y, Zhang Y, Sun X, Ye H, Li W (2008) Synthesis and characterization of polyurethane elastomers. J Elastom Plast 40:161–177
3. Gorrasi G, Tortora M, Vittoria V (2005) Synthesis and physical properties of layered silicates/polyurethane nanocomposites. J Polym Sci B 43:2454–2467
4. Velankar S, Cooper SL (2000) Microphase separation and rheological properties of polyurethane melts. 2. Effect of block incompatibility on the microstructure. Macromolecules 33:382–394
5. Kim CK, Bae SB, Ahn JR, Chung IJ (2008) Structure–property relationships of hydroxy-terminated polyether based polyurethane network. Polym Bull 61:225–233
6. Skarja GA, Woodhouse KA (2000) Structure–property relationships of degradable polyurethane elastomers containing an amino acid-based chain extender. J Appl Polym Sci 75:1522–1534
7. Woo GLY, Mittelman MW, Santerre JP (2000) Synthesis and characterization of a novel biodegradable antimicrobial polymer. Biomaterials 21:1235–1246
8. Hasirci N, Aksoy EA (2007) Synthesis and modifications of polyurethanes for biomedical purposes. High Perform Polym 19:621–637
9. d'Arlas BF, Rueda L, Caba K, Mondragon I, Eceiza A (2008) Microdomain composition and properties differences of biodegradable polyurethanes based on MDI and HDI. Polym Eng Sci 48:519–529
10. Marcos-Fernandez A, Abraham GA, Valentin JL, San Roman J (2006) Synthesis and characterization of biodegradable non-toxic poly(ester-urethane-urea)s based on poly(-caprolactone) and amino acid derivatives. Polymer 47:785–798
11. Gorna K, Gogolewski S (2003) Molecular stability, mechanical properties, surface characteristics and sterility of biodegradable polyurethanes treated with low-temperature plasma. Polym Degrad Stab 79:475–485
12. Heijkants GJC, Calck RV, Tienen TG, Groot JH, Buma P, Pennings AJ, Veth PH, Schouten AJ (2005) Uncatalyzed synthesis, thermal and mechanical properties of polyurethanes based on poly(caprolactone) and 1, 4-butane diisocyanate with uniform hard segment. Biomaterials 26:4219–4228
13. Hatakeyama T, Izuta Y, Hirose S, Hatakeyama H (2002) Phase transitions of lignin-based polycaprolactones and their polyurethane derivatives. Polymer 43:1177–1182
14. Wang W, Ping P, Chen X, Jing X (2007) Shape memory effect of poly(L-lactide)-based polyurethanes with different hard segments. Polym Int 56:840–846
15. Labow R, Sa D, Matheson L, Santerre J (2005) Polycarbonate-urethane hard segment type influences esterase substrate specificity for human-macrophage-mediated biodegradation. J Biomater Sci Polym Ed 9:1167–1177
16. McBane J, Santerre J, Labow R (2007) The interaction between hydrolytic and oxidative pathways in macrophage-mediated polyurethane degradation. J Biomed Mater Res 82A(4):984–994
17. Zapletalova T, Michielsen S, Pourdeyhimi B (2006) Polyether based thermoplastic polyurethane melt blown nonwovens. J Eng Fibers Fabr 1:62–72
18. Oprea S (2007) Synthesis and characterization of polyurethane-urea-acrylates: effects of the hard segments structure. J Appl Polym Sci 105(5):2509–2515

19. Fu BX, Hsiao BS, White H, Rafailovich M, Mather PT, Jeon HG, Phillips S, Lichtenhan J, Schwab J (2000) Nanoscale reinforcement of polyhedral oligomeric silsesquioxane (POSS) in polyurethane elastomer. Polym Int 49:437–440
20. Tang Y, Labow R, Santerre J (2001) Enzyme-induced biodegradation of polycarbonate-polyurethanes: dependence on hard-segment chemistry. J Biomed Mater Res 57:597–611
21. Erbil H (1997) Surface tension of polymers in handbook of surface and colloid chemistry. CRC Press, New York
22. Lligadas G, Ronda JC, Gali M, Cadiz V (2007) Polyurethane networks from fatty-acid-based aromatic triols: synthesis and characterization. Biomacromolecules 8(6):1858–1864
23. Zhang C, Ren Z, Yin Z, Qian H, Ma D (2008) Amide II and amide III bands in polyurethane model soft and hard segments. Polym Bull 60:97–101
24. Papadimtrakopoulos F, Sawa E, MacKnight WJ (1992) Investigation of a monotropic liquid crystal polyurethane based on biphenol, 2, 6-tolylene diisocyanate, and a six methylene containing flexible spacer. 2. IR spectroscopic phase characterization. Macromolecules 25:4682–4691
25. Chamberlim Y, Pascault JP (1984) Phase separation kinetics in segmented linear polyurethanes: relation between equilibrium time and chain mobility and between equilibrium degree of segregation and interaction parameter. J Polym Sci Polym Phys 22:1835–1844
26. Meng Q, Hu J, Zhu Y, Lu J, Liu Y (2007) Polycaprolactone-based shape memory segmented polyurethane fiber. J Appl Polym Sci 106:2515–2523
27. Li J (2006) High performance epoxy resin nanocomposites containing both organic montmorillonite and castor oil-polyurethane. Polym Bull 56:377–384
28. Oprea S (2008) Effect of the diisocyanate and chain extenders on the properties of the cross-linked polyetherurethane elastomers. J Mater Sci 43:5274–5281
29. Chang EJ, Kim HH, Huh JE, Kim IA, Seung KJ, Chung CP, Kim HM (2005) Low proliferation and high apoptosis of osteoblastic cells on hydrophobic surface are associated with defective Ras signaling. Exp Cell Res 303(1):197–206
30. Erbil HY (2006) Surface chemistry of solid and liquid interfaces. Blackwell, Oxford